http://www.uem.br/acta ISSN printed: 1806-2563 ISSN on-line: 1807-8664

Doi: 10.4025/actascitechnol.v35i2.11791

Method for determining the footprint area of air temperature and relative humidity

Elis Dener Lima Alves^{1*} and Marcelo Sacardi Biudes²

¹Escola de Engenharia de São Carlos, Centro de Recursos Hídricos e Ecologia Aplicada, Universidade de São Paulo, Rod. Domingos Innocentini, Km 13, 13530-000, Itirapina, São Paulo, Brazil. ²Instituto de Física, Universidade Federal de Mato Grosso, Cuiabá, Mato Grosso, Brazil. *Author for correspondence. E-mail: elisdener@usp.br

ABSTRACT. Despite the numerous studies in the area of urban climatology, there is still a relevant gap in this area corresponding to the demarcation of the footprint area on a variable. Various authors arbitrarily delimit this area without a prior study, which leads to significant errors in the results. In recent years, a variety of models to estimate the footprint area was presented mainly with stochastic and analytical approaches, usually expensive. Thus this article aimed to develop a methodology based on geostatistics for inference of the footprint area for temperature and relative humidity. By using geostatistics it was possible to observe that the radius of footprint had a temporal variation (between times and days) and spatial variation (between points), pointing out the great importance in assessing the footprint area. However, for a better analysis of this method we suggest to model the anisotropy in future studies, because the footprint area behaves like an ellipse with different radii at different directions. And for this, it is necessary to collect data with a regular distribution within a mesh.

Keywords: footprint area, semivariogram, air temperature, relative humidity.

Método para determinação da área de influência da temperatura do ar e umidade relativa

RESUMO. Na área de climatologia urbana, há diversos estudos, no entanto, ainda há uma lacuna pertinente nesta área que corresponde à delimitação da área de influência sobre uma variável. Vários autores, arbitrariamente, delimitam essa área sem estudo prévio da mesma, o que acaba ocasionando erros significativos nos resultados. Nos últimos anos, uma variedade de modelos para se estimar a área de influência foi apresentada, principalmente, com abordagens analíticas, e estocásticas. Estas abordagens são demasiadamente onerosas. Diante disto, este artigo tem como objetivo propor uma metodologia baseada na geoestatística para inferência da área de influência para a temperatura e umidade relativa do ar. Os resultados mostraram que com o uso da geoestatística foi possível observar que o raio de influência possui variação temporal (entre os horários e dias) e variação espacial (entre os pontos), com isso percebeu-se a grande importância na aferição da área de influência. Contudo, para melhor análise deste método sugere-se às pesquisas futuras que se modele a anisotropia, porque a área de influência se comporta como elipse com diferentes raios em diferentes direções, e para isso faz-se necessário coleta de dados distribuídos regularmente dentro de uma malha.

Palavras-chave: área de influência, semivariograma, temperatura do ar, umidade relativa.

Introduction

The concept of footprint (influence area) was introduced by Pasquill (1972) who observed that measurements taken at a certain point could be accepted as representative of an adjacent uneven surface.

A sensor placed above a surface *sees* only part of their surroundings. This is called as footprint area of the instrument (OKE, 2006). A conceptual illustration of this catchment area is presented in Figure 1.

Several studies have been performed in the urban climatology area, but there is a gap corresponding to

the determination of a footprint relative to a variable. Some authors arbitrarily delimit this area without a prior study, such as Costa et al. (2006) that delimited a 150 m-radius to the north and west directions, and a 350 m-radius to south and east directions, so that the resultant radius had 500 m, and Gomes and Lamberts (2009) that delimited a 150 m-radius.

However Duarte and Serra (2003) and Rego and Meneguetti (2011) stressed that there is no consensus among studies on urban climate about the footprint radius of climate measurement, especially because the footprint of a sensor is not

symmetrically distributed around it (according to Figure 1). It is an elliptical shape aligned on the opposite direction of the wind.

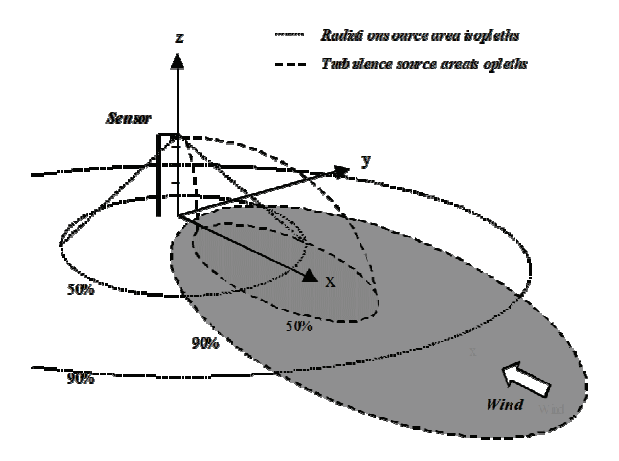


Figure 1. Conceptual representation of the catchment area that contributes to sensors of radiation and turbulent flows. If the sensor is a radiometer, 50 or 90% of flow originates from the area inside the respective circle. If the sensor is responding to a property of the turbulent transport, 50 or 90% of the signal comes from the area inside the respective ellipse. These are dynamic, so that they are oriented in the direction of the wind. Adapted from Oke (2006).

According to Oke (2006) the footprint of temperature and relative air humidity has on average 500 m of radius. It depends on the height at which the sensor measurements were made, surface roughness, and primarily on the direction and speed of wind (OKE, 2006).

Grimmond (2006) argues that the measurement footprint is a function of the variable under observation, method used, location of the equipment, nature of the surface and in some cases meteorological conditions as well.

A great problem to define the footprint area of a sensor is because it is highly variable over space and time, and methods for its estimation are in most cases, much complex.

A series of studies have addressed the local advection, i.e., the contribution of sources located at a windward distance from the collection point, through analytical solutions of diffusion equations.

In recent years, various models have been presented to estimate the footprint, especially with analytical and stochastic approaches. A detailed analysis of these approaches and their applications can be found in Schmid (2002).

Schmid (2002), Kljun et al. (2004) used twodimensional diffusion equations to simulate the footprint edge, but these methods are expensive and difficult to reproduce. Thus Schuepp et al. (1990) identified an urgent need for solutions able to give magnitude order to this footprint, from methods able to estimate it and to be reproducible in studies on urban climatology.

This study aimed to develop a methodology based on geostatistics for inference of footprint of temperature and relative humidity.

Geostatistics

The geostatistics includes the analysis of spatial and/or temporal phenomenon, and has its origins in the mining sector. Currently it is used to analyze and infer values. These values are implicitly correlated with others, and the study of such correlation is called structural analysis or variogram modeling.

The success and assumptions of geostatistical techniques are based on the *Theory of Regionalized Variables*. The regionalized variable is a variable distributed in space (or time). The theory states that a measure can be seen as an achievement of a random function (or random process, or random field, or stochastic process). This theory consolidates the foundation of the geostatistics.

According to Burrough (1987) the spatial variation of a regionalized variable can be expressed by the summation of three components: a) a structural component associated with a constant mean value or to a constant tendency; b) a random component, spatially correlated; and c) a random noise or residual error.

If x is a position on one, two, or three dimensions, then the value of the variable Z, in x, is given by Burrough (1987):

$$Z(x) = m(x) + \varepsilon'(x) + \varepsilon''$$
 (1)

where:

m(x) is a deterministic function that described the structural component of Z into x;

 $\varepsilon'(x)$ is an stochastic term, which varies locally and is spatially dependent on m(x);

 ε'' is an uncorrelated random noise, with normal distribution with mean zero and variance σ^2 .

Variogram

The variogram allows representing quantitatively the variation of a regionalized phenomenon. Considering two regionalized variables, X and Y, where X = Z(x) and Y = Z(x+h), relative to the same attribute (e.g. zinc content in the soil) measured in two different positions (DRUCK et al., 2004), as shown in Figure 2.

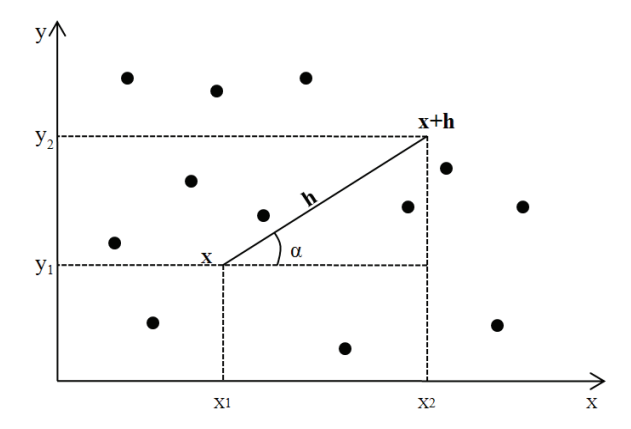


Figure 2. Sampling in two dimensions.

where:

x is a position in two dimensions, with components (x_i, y_i) ;

h is a distance vector (modulus and direction) that separates the points.

The dependence level between these two regionalized variables, X and Y, is represented by the variogram, $2\gamma(h)$, which is defined as the mathematical expectation of the square of the difference between the values of points on space, separated by the distance vector h, i.e.:

$$2\gamma(h) = E\{[Z(x)-Z(x+h)]^2\} = Var[Z(x)-Z(x+h)]$$
 (2)

With a sample $z(x_i)$, i=1, 2, ..., n, the variogram can be estimated by:

$$2\hat{\gamma}(h) = \frac{1}{N(h)} \sum_{i=1}^{N(h)} [z(x_i) - z(x_i + h)]^2$$
 (3)

where:

2 $\hat{y}(h)$ is the estimated variogram;

N(h) is the number of pairs of values measured, $z(x_i)$ and $z(x_i+h)$, separated by a distance vector h;

 $z(x_i)$ and $z(x_i+h)$ are values of the *i*-th observation of the regionalized variable, collected on the points x_i and x_i+h (i=1,...,n), separated by the vector h.

Many authors define variogram different from the Equation 2, considering what is usually referred to as semivariogram, given by:

$$\gamma(h) = \frac{1}{2} E\{ [Z(x) - Z(x+h)]^2\} = \frac{1}{2} Var[Z(x) - Z(x+h)]$$
 (4)

Similarly, the semivariogram function can be estimated as:

$$\hat{\gamma}(h) = \frac{1}{2N(h)} \sum_{i=1}^{N(h)} [z(x_i) - z(x_i + h)]^2$$
 (5)

Semivariogram parameters

The Figure 3 shows an experimental semivariogram with characteristics close to ideal. Its pattern represents the expected from field data, i.e., the differences $\{Z(x_i) - Z(x_i + h)\}$ progressively decrease as the distance h between them decreases. It is expected that observations geographically closer have more similar behavior than those separated by greater distances. In this way, it is expected that $\gamma(h)$ increases with the distance h (DRUCK et al., 2004).

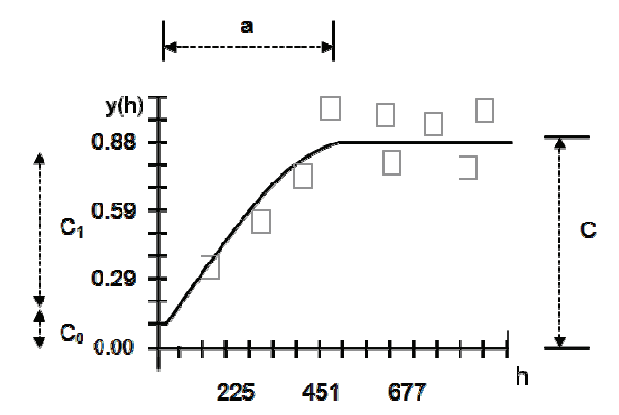


Figure 3. Example of an experimental semivariogram.

where:

Range (a): distance within which samples are spatially correlated;

Sill (C): is the semivariogram value corresponding to its range (a). From this point on, there is no longer spatial dependence between the samples, because the variance of the difference between pairs of samples (Var[Z(x) - Z(x+h)]) becomes invariant with the distance.

Nugget Effect (C_0): ideally, $\gamma(0) = 0$. However in practice as h tends to zero, $\gamma(h)$ approaches a positive effect called Nugget Effect (C_0), which reveals the semivariogram discontinuity for distances smaller than the shortest distance between samples. Part of this discontinuity can be also due to measurement errors (Isaaks and Srivastava, 1989), but it becomes impossible to quantify if the largest contribution arises from measurement error or from the small scale variability not captured by the sampling.

Contribution (C_1) : is a parameter of the fit model, presented below, whose value is the difference between the sill (C) and the Nugget Effect (C_n) .

Theoretical models

The chart of the experimental semivariogram $\hat{y}(h)$, calculated with the Equation (5) is formed by a series of values, as illustrated in the Figure 3, on which the objective is to fit a function. It is important that the fit model represents the tendency of $\hat{y}(h)$ in relation to h.

The fit procedure is not direct and automatic, such as in a regression, but interactive because in this process the interpreter makes a first setting and checks the adequacy of the theoretical model. Depending on the obtained fit, the model may or may not be reset, until achieving a satisfactory model (DRUCK et al., 2004).

Models presented herein are considered basic, called isotropic models and classified into two types: models with sill and models without sill. The first are referred in geostatistics as transitive models. Some transitive models reach the sill (*C*) asymptotically. For these models, the range (*a*) is arbitrarily defined as the distance corresponding to 95% of the sill. The second type models do not reach the sill, and continue increasing with increasing distance. These models are used to model phenomena with infinite capacity of dispersion. The most used transitive models are: spherical model, exponential model, and Gaussian model (DRUCK et al., 2004). These models are presented in Figure 4 with the same range (*a*).

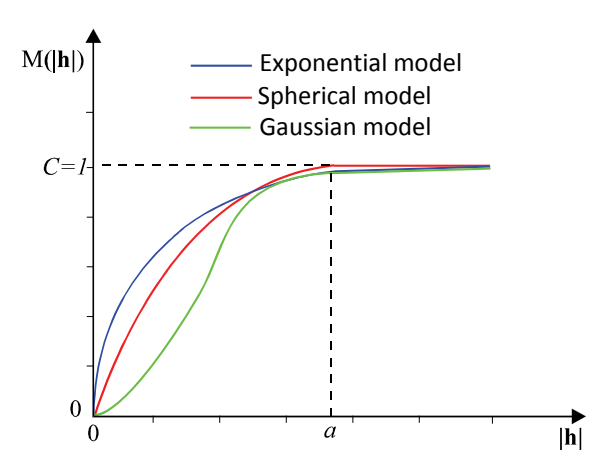


Figure 4. Graphic representation of normalized transitive models.

Material and methods

In order to infer the footprint, global semivariograms were calculated with data collected through two mobile transects that sought to include different patterns of land occupation in the Federal University of Mato Grosso (UFMT), campus of Cuiabá, and local semivariograms for seven points. The location of the UFMT and respective transects can be observed in the Figure 5.



Figure 5. Location of the UFMT, of the transects 1 and 2 of the discussion points.

Data collection

Data were gathered on April 21, 23, 24, 25, 27 and 29, 2010, at three times, 8, 14, and 20h. The choice of these times was due to the recommendation of the World Meteorological Organization (WMO) that the main meteorological observation should occur at 0, 6, 12 and 18h (Greenwich Meridian Time - GMT), corresponding to 2, 8, 14 and 20h, local time, including representative periods of a day, morning, afternoon, and evening. Thus, by the end of each day, the meteorological characteristics of each period were registered, which were required for estimating the footprint.

For the transects, it was used two thermohygrometers (HT-4000) and two GPS (Global Positioning System) fitted to register and store variable data (temperature, humidity and coordinates) every 10 seconds. Given the mean velocity along the transect, registered by the GPS receptor, 1.4 m s⁻¹, each transect point is at a mean distance of 14 m of other adjacent points. The course of the transects 1 and 2 was approximately 1.86 and 2.57 km, recording on average 132 and 183 points, respectively. Therefore, totaling on average 315 data of temperature and relative humidity georeferenced.

Results and discussion

Global semivariogram

As observed in Figure 5, the data collection was distributed into rows (transects) meaning that nothing can be stated about anisotropy (different ranges for different directions) and it is considered that the footprint is isotropic (same range for different directions) corresponding to a circle.

For analysis purposes, the footprint radius was used, and the footprint can be calculated from the circle area:

$$A = \pi r^2 \tag{6}$$

In order to attain the value of the range corresponding to the influence radius of the entire study area, we used for the calculation of global semivariograms all the data collected in the transects.

Thus it was possible to observed that for all global semivariograms of temperature and relative humidity, the model that better fitted the data was the Gaussian, according to Figures 6 and 7. In the

Figure 6, the nugget effect C_0 was close to zero in all semivariograms, indicating no data variability in spacing smaller than studied (14 m). The value of the range (footprint radius) of air temperature (128.8 m), at 8h, was above the range of relative humidity (74.6 m). At 14h, the range of temperature continued above the humidity. During the night, this is reversed, i.e. temperature and humidity presented ranges of 193.9 and 225.8 m, and for this period, data variability in the semivariograms was similar.

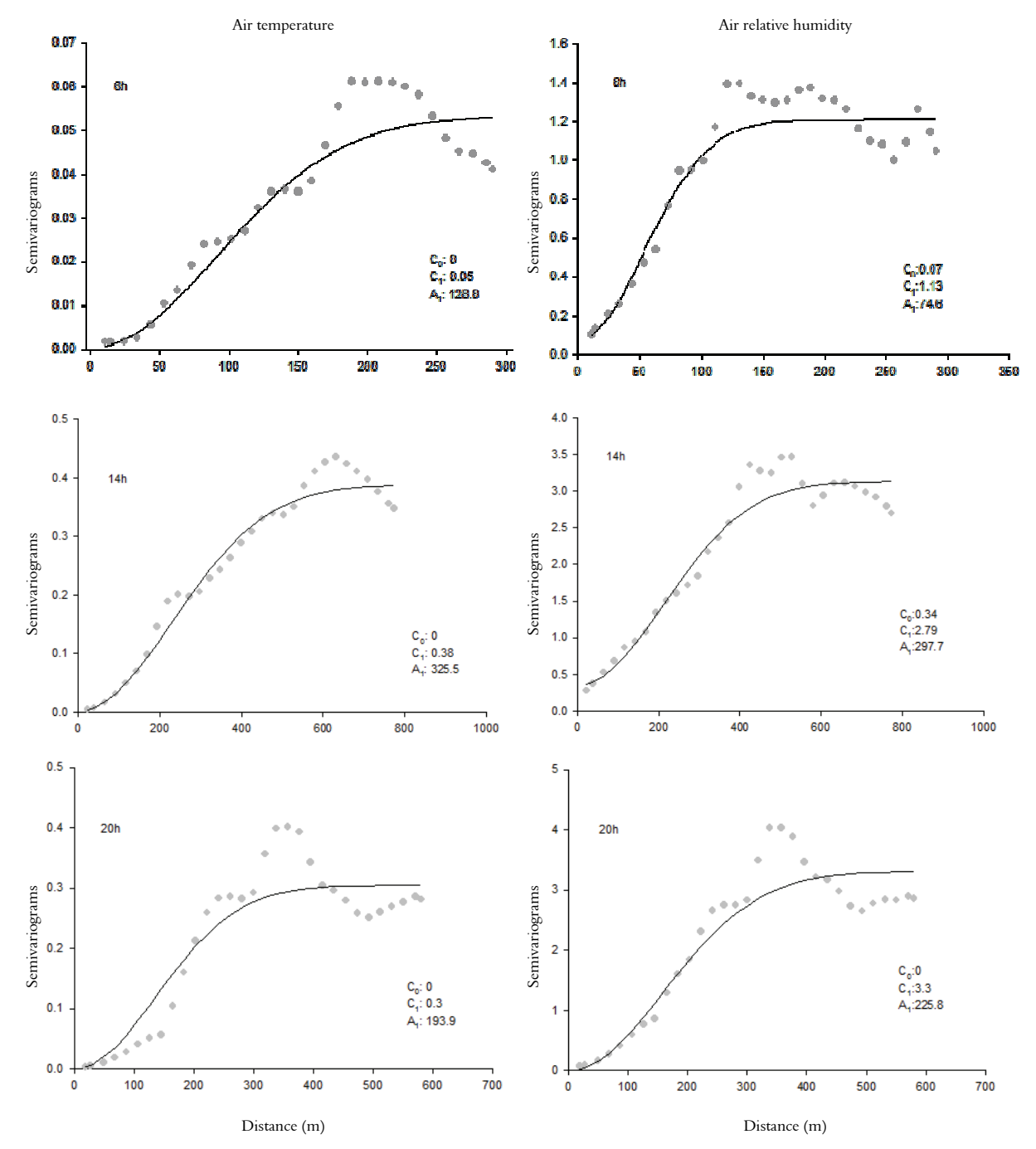


Figure 6. Global semivariograms of temperature and humidity on April 21st, at 8, 14 and 20h.

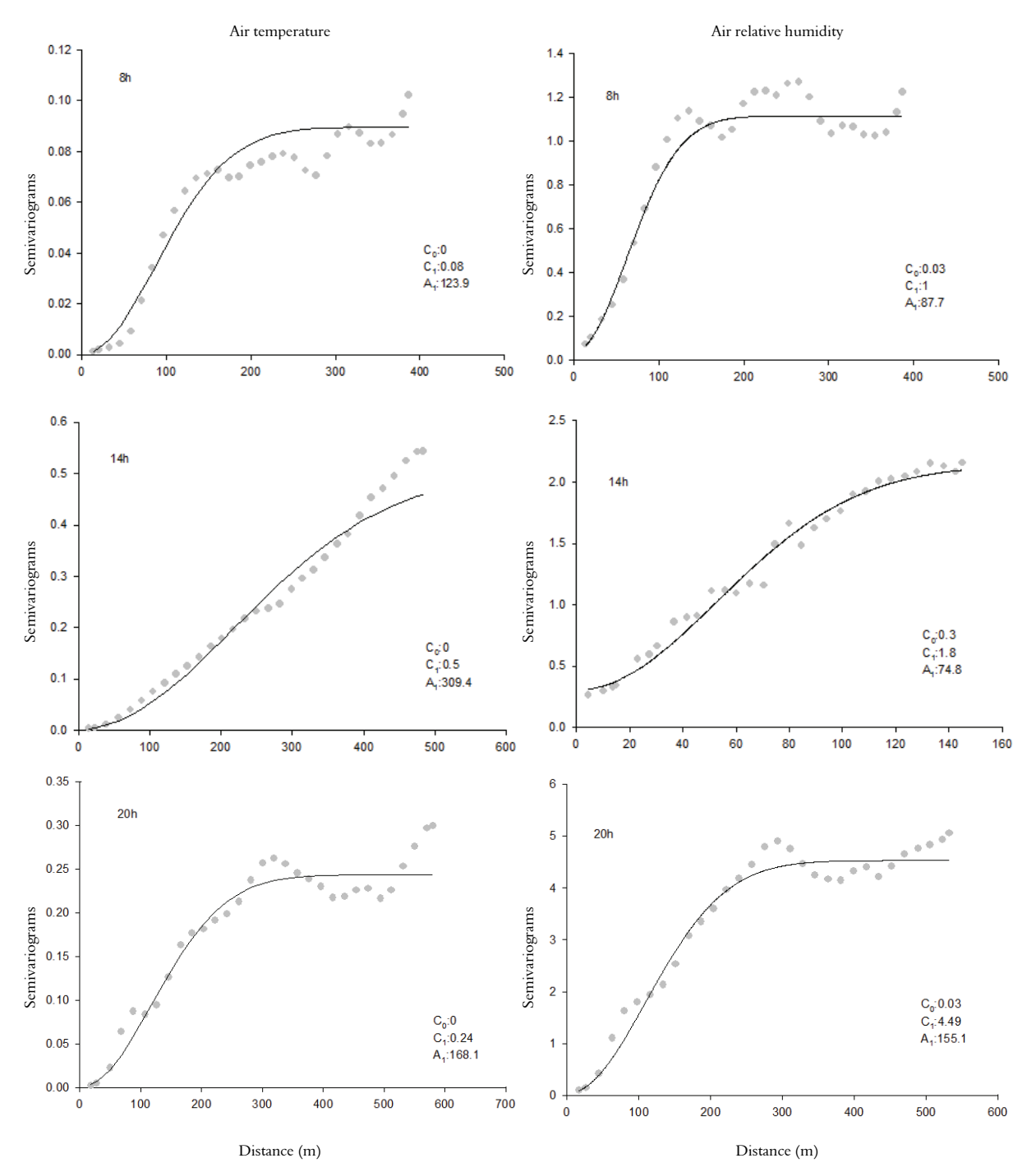


Figure 7. Global semivariograms of temperature and humidity on April 25th, at 8, 14 and 20h.

In agreement with that presented by global semivariograms of the Figure 6 for April 21st, the semivariogram of the Figure 7 for air temperature on day 25 presented a greater range (123.9 m) than the humidity (87.7 m) by the morning (8h), and this was kept in the afternoon, with ranges of 309.4 and 74.8 m for temperature and relative humidity, respectively. However, at 20h the influence radius continued to be above humidity, in the disagreement with presented by

Figure 6. It can be observed similar behavior of semiovariograms variability at 14 and 20h, but with different magnitudes.

On the day 21 (Figure 6) and on the day 25, there was a great variability in the value of range, presenting on the day 21, at 14h for air temperature the highest value with 325.5 m, as well as for humidity (297.7 m). On the day 25, the highest value of range for temperature occurred only at 14h, with value of

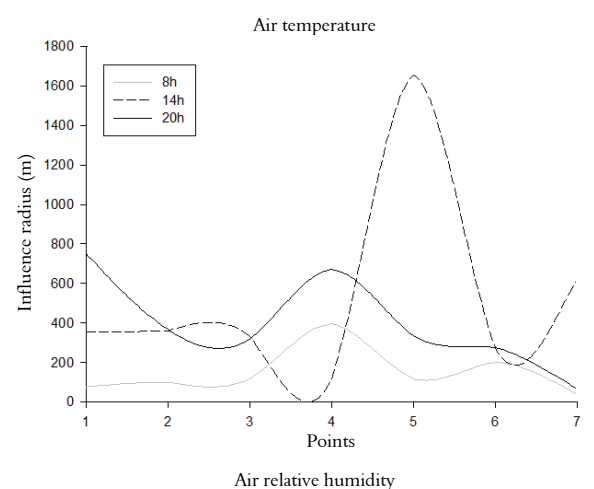
309.4 m, but for the relative humidity the highest value occurred at 20h (155.1 m).

Nevertheless, the ranges (influence radius) found by means of global semivariograms were below the radius preset by Oke (2006), but the same author affirms that this is quite variable and influenced by several factors.

Local semivariogram

In order to verify the spatial variability of the footprint the calculation of the semivariograms were performed in seven points distributed throughout the study area.

In Figures 8 and 9, a great spatial variability was observed for the influence radius, as well as a great variability in time. The behavior of the influence radius for air temperature was similar at 8 and 20h, with a high value in the period of 14h at the point 5 (1,700 m) and low value at the point 4 (90 m) (Figure 8). In the Figure 9, for the temperature the point 6 presented at 14h the highest value (790 m) and the point 2, the lowest value at 8h (80 m).



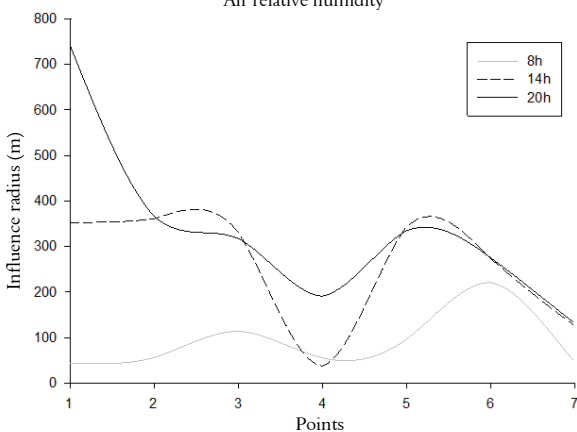
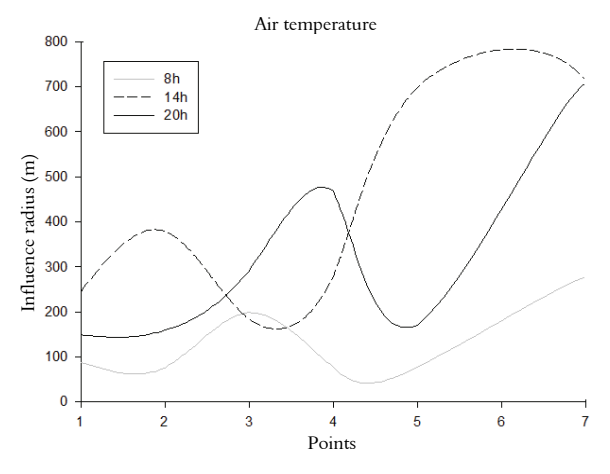


Figure 8. Spatial variability of the influence radius for temperature and relative humidity on April 21st.

When compared the variation of the influence radius of relative humidity in Figure 8 and 9 it is observed a great difference, because in the Figure 8 the lower values are observed at the point 4. In the Figure 9, the point 4 obtained the largest influence radius of the day.



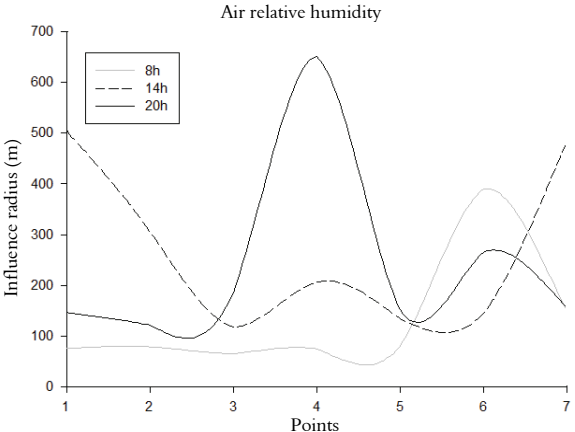


Figure 9. Spatial variability of the influence radius for temperature and relative humidity on April 25th.

Conclusion

With the determination of the influence radius it was possible to verify that it has varied between the hours and days (temporal variation) and between points (spatial variation), evidencing its complexity that varies over space and time.

The use of geostatistical procedures, in this case the semivariogram, was effective to determine the footprint.

In future studies it is suggested to model the anisotropy, since according to Oke (2006) the footprint behaves as an ellipse with different radii in different directions, and therefore it necessary collection of data evenly distributed within a network.

Therefore it is advisable to perform data collections at other times to make a more detailed analysis of intraday variations of the footprint.

References

BURROUGH, P. A. **Principles of geographical information systems for land resources assessment**. Oxford: Clarendon Press, 1987.

COSTA, A.; LABAKI, L.; ARAÚJO, V. Medições de campo na área urbana: o desafio da padronização. **Revista de Urbanismo e Arquitetura**, v. 7, n. 1, p. 26-31, 2006. DUARTE, D.; SERRA, G. Padrões de ocupação do solo e microclimas urbanos na região de clima tropical continental brasileira: correlações e proposta de um indicador. **Ambiente Construído**, v. 3, n. 2, p. 7-70, 2003

DRUCK, S.; CARVALHO, M. S.; CÂMARA, G.; MONTEIRO, A. V. M. **Análise espacial de dados geográficos**. Brasília: Embrapa, 2004.

GOMES, P. S.; LAMBERTS, R. O estudo do clima urbano e a legislação urbanística: considerações a partir do caso Montes Claros, MG. **Ambiente Construído**, v. 9, n. 1, p. 73-91, 2009.

GRIMMOND, C. S. B. Progress in measuring and observing the urban atmosphere. **Theoretical and Applied Climatology**, v. 84, n. 1-3, p. 3-22, 2006.

KLJUN, N.; CALANCA, P.; ROTACH, M. W.; SCHMID, H. P. A simple parameterization for flux footprint predictions. **Boundary-Layer Meteorology**, v. 112, n. 3, p. 503-523, 2004.

OKE, T. R. Initial guidance to obtain representative meteorological observations at urban sites. **IOM Report no. 81, WMO/TD**, n. 1250, p. 1-47, 2006.

PASQUILL, F. Some aspects of boundary layer description. **Quarterly Journal of the Royal Meteorological Society**, v. 98, n. 417, p. 469-494, 1972.

REGO, R. L.; MENEGUETTI, K. S. A respeito de morfologia urbana. Tópicos básicos para estudos da forma da cidade. **Acta Scientiarum. Technology**, v. 33 n. 2, p. 123-127, 2011.

SCHUEPP, P. H.; LECLERC, M. Y.; MACPHERSON, J. I.; DESJARDINS, R. L. Footprint prediction of scalar fluxes from analytical solutions of the diffusion equation. **Boundary-Layer Meteorology**, v. 50, n. 1-4, p. 355-373, 1990.

SCHMID, H. P. Footprint modeling for vegetation atmosphere exchange studies: a review and perspective. **Agricultural and Forest Meteorology**, v. 113, n. 1-2, p. 159-183, 2002.

Received on November 24, 2010. Accepted on August 1, 2012.

License information: This is an open-access article distributed under the terms of the Creative Commons Attribution License, which permits unrestricted use, distribution, and reproduction in any medium, provided the original work is properly cited.